A combination of genome reduction and promoter engineering can enhance surfactin production by *Bacillus amyloliquefaciens* LL3

Fang Zhang
Nankai University
Kaiyue Huo
Nankai University
Xingyi Song
Nankai University
Yufen Quan
Nankai University
Weixia Gao
Tianjin University of Science and Technology
Shufang Wang
Nankai University
Chao Yang (yangc20119@nankai.edu.cn)
Nankai University https://orcid.org/0000-0002-7607-6621

Research

Keywords: Bacillus amyloliquefaciens, Genome reduction, promoter engineering, surfactin production

Posted Date: September 11th, 2020

DOI: https://doi.org/10.21203/rs.3.rs-41198/v2

Version of Record: A version of this preprint was published at Microbial Cell Factories on December 7th, 2020. See the published version at https://doi.org/10.1186/s12934-020-01485-z.

Abstract

Background: Genome reduction and metabolic engineering have emerged as intensive research hotspots for constructing the promising functional chassis and various microbial cell factories. Surfactin, a lipopeptide-type biosurfactant with broad spectrum antibiotic activity, has wide application prospects in anticancer therapy, biocontrol and bioremediation. *Bacillus amyloliquefaciens* LL3, previously isolated by our lab, contains an intact *srfA* operon in the genome for surfactin biosynthesis.

Results: In this study, a genome-reduced strain GR167 lacking ~4.18% of the *B. amyloliquefaciens* LL3 genome was constructed by deleting some unnecessary genomic regions. Compared with the strain NK-1 (LL3 derivative, Δ*upp*ΔpMC1), GR167 harbored faster growth rate, higher transformation efficiency, increased intracellular reducing power level and higher heterologous protein expression capacity. Furthermore, the promising chassis GR167 was engineered for enhanced surfactin production. Firstly, the iturin and fengycin biosynthetic gene clusters were deleted from GR167 to generate GR167ID. Subsequently, two promoters PR_{suc} and PR_{tpxi} from LL3 were obtained by RNA-seq and promoter strength characterization, and then they were individually substituted for the native *srfA* promoter in GR167ID to generate GR167IDS and GR167IDT. The best mutant GR167IDS showed a 678-fold improvement in the transcriptional level of the *srfA* operon relative to GR167ID, and it produced 311.35 mg/L surfactin, with a 10.4-fold increase relative to GR167.

Conclusions: The genome-reduced strain GR167 was advantageous over the parental strain in several industrially relevant physiological traits assessed and it was highlighted as a promising chassis for further genetic modification. In future studies, further reduction of the LL3 genome can be expected to create high-performance chassis for synthetic biology applications.

Background

With the development of systems and synthetic biology, numerous studies have focused on the design and construction of the optimal functional microbial chassis with reduced genomes and superior physiological characteristics [1, 2]. Moderate genome reduction can create synthetic biology chassis with optimized genomic sequences, efficient metabolic regulatory networks and superior cellular physiological characteristics [3-5]. So far, several model microorganisms, such as *Escherichia coli* [6], *Bacillus subtilis* [7, 8] and *Pseudomonas putida* [9], have been intensively researched for minimal genome construction due to their clear genetic background and efficient genome editing approaches.

Surfactin, which contains a ring-shaped heptapeptide and a β-hydroxy fatty acid chain with 13–16 carbons, is a cyclic lipopeptide (CLP) biosurfactant with broad-spectrum antibiotic activity and mainly produced by *Bacillus* sp. via multifunctional non-ribosome peptide synthases (NRPSs) encoded by the *srfA* operon containing four open reading frames (*srfAA*, *srfAB*, *srfAC* and *srfAD*) [10, 11]. Surfactin is one of the most promising green biosurfactants for its extraordinary activities (i.e., anti-viral, anti-tumor and

anti-bacterial), which can be used in various files, such as food processing, pharmaceuticals, oil recovery, and environmental governance [12-14].

In recent years, several metabolic engineering strategies have been proposed for enhancing biosurfactant production, mainly including promoter engineering [15-17], the reduction of by-product formation [11], the enhancement of the precursor supply [2], the improvement of biosurfactant transmembrane efflux [18], and the modification of global regulatory factors [19]. Among which, promoter engineering is highlighted as a powerful tool for enhancing the titer of biosurfactants. For example, the titer of iturin A was increased from an undetectable level to 37.35 mg/L by inserting a strong promoter C2up into upstream of the *itu* operon in *B. amyloliquefaciens*. [17] In another study, the titer of surfactin in *B. subtilis* was elevated from 0.07 g/L to 0.26 g/L by the replacement of the native *srfA* promoter with a constitutive promoter P_{veg} [20]. In addition to the natural promoters, Jiao et al [16] developed a chimeric promoter Pg3 for driving the synthesis of surfactin, resulting in a 15.6-fold increase in the titer of surfactin relative to the wild-type *B. subtilis* THY-7. However, efficient promoters need to be explored for the enhancement of biosurfactants production by members of the genus *Bacillus*.

Currently, endogenous promoters are highlighted as promising candidates for improved production of bacterial secondary metabolites [21]. For example, 14 endogenous promoters identified from *Streptomyces albus* J1074 by RNA-seq and reporter assays were successfully used to activate a cryptic gene cluster in *S. griseu* [22]. In another study, four endogenous promoters identified from *S. coelicolor* M145 by RNA-seq and reporter assays were used to activate cryptic biosynthetic clusters for jadomycin B production in *S. venezuelae* ISP5230 [5].

B. amyloliquefaciens LL3 was isolated initially for poly-γ-glutamic acid (γ-PGA) production by our lab, and whole genome of LL3 is currently available in the GenBank database (accession no. NC_017190.1) [23]. LL3 has a genomic size of 3,995,227 bp with an average G+C content of 45.7% and a circular plasmid (pMC1) of 6,758 bp. In particular, an intact *srfA* operon was found in the genome of LL3, suggesting the capability for surfactin biosynthesis. The essential genes and genomic islands (GIs) in LL3 were also identified by the Essential Genes Database (http://tubic.tju.edu.cn/deg/) and GIs Analysis Software (http://tubic.tju.edu.cn/GC-Profile/). Previously, a marker-free large fragments deletion method was well established inLL3 [24]. Therefore, previous studies have laid a foundation for genome reduction and enhanced surfactin production in LL3.

In this study, a genome-reduced strain GR167 was constructed from *B. amyloliquefaciens* NK-1 (LL3 derivative, Δ*upp*ΔpMC1) [25] and evaluated as a promising chassis for several physiological traits. Furthermore, GR167 was engineered using metabolic engineering strategies for enhanced surfactin production. Strategies designed for enhancing surfactin production in *B. amyloliquefaciens* are shown in Fig. 1.

Results And Discussion

Construction of genome-reduced *B. amyloliquefaciens* strains

To adapt to the adverse environmental conditions, there is a common mechanism horizontal gene transfer (HGT) among microorganisms, enabling host bacteria to acquire larger DNA segments, i.e., GIs, the G+C contents of which are significantly different from that of the core genome [26]. GIs usually carry some functional genes related to pathogenicity and antibiotic resistance, leading to the emergence of multiple resistant bacteria by HGT [27]. In addition, there are latent secondary metabolic biosynthesis gene clusters scattered across the LL3 genome, which may increase the metabolic burden on cells and the purification cost of target products [28]. Consequently, to streamline the genome of LL3, the GIs containing putative protein genes, antibiotic biosynthesis genes and prophage protein genes, where the G+C contents deviate significantly from 45.7%, were selected as the knockout targets. Besides, the gene clusters *eps*, *bae* and *pgsBCA* responsible for the biosynthesis of extracellular polysaccharides, bacillaene and γ-PGA, respectively, which consume more energy and substrates, were also deleted from the LL3 genome. The detailed information on the deleted regions is summarized in Tables S1 and S2. The schematic diagram for deletion of large genomic segments in LL3 is presented in Figure S1. Overall, a genome-reduced strain GR167 lacking ~4.18% of the LL3 genome was generated from NK-1 via a markerless deletion method [24]. The exact coordinates (G1 to G6) of the deleted regions on chromosome and the physical map of the endogenous plasmid pMC1 are shown in Figs. 2a and b, respectively.

Deleting redundant genes from a bacterial genome is expected to create superior chassis cells for the industrial production of valuable bio-based chemicals. Due to the existence of unannotated genes in the LL3 genome and lack of insight into the interactions among known genes, several industrially-relevant physiological traits were carried out in GR167 and GR94 (lacking ~2.36% of the LL3 genome) to evaluate whether an ideal chassis can be produced via genome reduction.

Improved growth parameters of the genome-reduced strain GR167

To evaluate the effect of non-essential genomic sequences on cell growth, the growth profiles of GR94, GR167 and the parental NK-1 strain were detected by following the optical density (OD_{600}) of cells cultured in both poor (M9 medium) and rich (LB medium) conditions. As shown in Figs. 3a and b, obviously, whether incubated in LB or M9 medium, GR167 grew faster and yielded higher biomass with approximately 1.5 and 1.2-fold higher at the plateau phase than that of NK-1, respectively. By contrast, GR94 grew poorly in both media, and which started to grow exponentially 3 h behind the other two strains when cultivated in M9 medium (Fig. 3b). The maximum specific growth rate (μ_{max}) of the strains was further determined during exponential growth. GR167 showed a 23.7% increase and GR94 showed a 17% decrease in μ_{max} when cultured in LB medium (Fig. 3c). No significant difference was observed between GR94 and the parental strain in μ_{max} when grown in M9 medium, while GR167 exhibited 67% increase (Fig. 3d).

During the evolution of the bacteria, various behaviors (e.g., horizontal gene transfer, HGT) enlarged the genome size, which might be harmful to cell growth because of the additional consumption for the expression of new substances. Nevertheless, the newly acquired sequences were subsequently optimized (e.g., mutation) to achieve the growth recovery [29]. Hence, it is hard to say whether the removal of the dispensable genomic sequences is advantageous or disadvantageous for the growth fitness of bacteria. Given that the genomic sequence evolution, the difference growth profiles of GR94 and GR167 might be associated with the deleted regions disturbed the genes distribution in LL3 genome and caused growth changes. Overall, deletion of ~4.18% of the LL3 genome did not affect cellular viability of GR167. However, the growth of GR94 was severely inhibited. The amount of removed DNA in GR167 was ~ 74 kb more than that in GR94 (Table S1), because many genes were removed simultaneously and which contains a large number of hypothetical protein-encoding genes with unknown functions (Table S2), it is difficult to determine which single gene knockout or which few gene interactions endowed GR167 with superior growth fitness.

Genome reduction can improve transformation efficiency of GR167

An ideal chassis cell is expected to possess the excellent capacity to take up exogenous plasmids. When transformed with plasmid pHT01, GR167 surpassed the transformation efficiency of the parental strain NK-1 by about 137%, in contrast, the transformation efficiency of GR94 was significantly lower than that of its parental strain (Fig. 3e). Since GR167 exhibits higher growth rate than NK-1, in order to explore whether the numbers of colonies observed following plating of the transformed bacteria be biased by faster propagating GR167 cells, the competent cells (100 μL) of the two strains without added plasmid DNA were electroporated, recovered and spread on LB agar plates, followed by cell count. Interestingly, there was rarely difference in the numbers on the plates, which indicates that the enhancement of transformation efficiency of GR167 was benefited from the better DNA uptake state during electroporation. For the transformation efficiency was a synergistic effect caused by many factors [30], it is difficult enough to pinpoint individual removed genes that are exactly affect the observed results in GR94 and GR167.

Genome reduction can increase intracellular reducing power and the expression capacity of heterologous protein

The intracellular reducing power (NADPH/$NADP^+$), which is indispensable for basic anabolic processes [31], was measured in this study. The intracellular NADPH/$NADP^+$ ratio of GR167 increased by 21.4% compared to the parental strain, the value of GR94 was slightly improved but with no significant difference with NK-1 (Fig. 3f). The removal of gene cluster (*pgsBCA*) for γ-PGA biosynthesis, which has been deleted in GR167 but not in GR94 (Table S1), might be benefited to the enhanced reducing power of GR167 for which synthesis is NADPH-consumable [32]. The improvement of intracellular reducing power

level may be beneficial for GR167 to act as an ideal chassis for enhanced production of secondary metabolites.

Besides, an ideal chassis is expected to possess high heterologous protein expression capacity. In previous studies, green fluorescent protein (GFP) was selected as a model heterologous protein in genome-reduced *P. putida* KT2440 mutants, and the GFP fluorescence per biomass unit was act as the expression capacity of heterologous protein [9, 33]. In this study, GFP was also selected as a heterologous protein, and which expression was evaluated at transcriptional and production levels by quantitative real-time PCR (RT-qPCR) and the fluorescence intensity. As shown in Fig. 3g, when transformed with plasmid pHT-P_{43}-*gfp*, the relative fluorescence intensity of GR167 was obviously higher (~50.4%) than that of GR94 and NK-1. Moreover, the transcription of *gfp* was also increased in GR167 though the gene was controlled under the same promoter P_{43}. By analyzing the genomic list (Table S2), the deleted regions in GR167 contain some transcriptional regulators and amounts of hypothetical proteins, they may form negative regulation with the regulatory factors of the P_{43} promoter or transcription complexes, weakening the transcription of *gfp* in the other two experimental strains. Overall, the reduced genome in GR167 has a positive effect on the expression capacity of heterologous protein.

Genome reduction can improve the metabolic phenotype

To further evaluate the difference in the metabolic potential of *B. amyloliquefaciens*, the GEN III MicroPlate™ was used to test and analyze the overall utilization of the substrates by both strains NK-1 and GR167. There are 71 carbon sources in the MicroPlates, 23 of which could be better utilized by both strains, especially L-Aspartic Acid, Citric Acid, L-Malic Acid, Glycerol, L-Glutamic Acid, and L-Lactic Acid, and among which, GR167 showed a better metabolic capacity than NK-1 except Glycerol (Table 1). This indicated that these substrates are the preferred carbon sources used by the *B. amyloliquefaciens* LL3 and its derivatives during their respiration, moreover, the genome reduction could improve the capacity of LL3 to metabolite certain substrates.

Use of genome-reduced strain GR167 as a starting strain for surfactin production

Surfactin is synthesized by the non-ribosomal peptide synthetase (NRPS) encoded by *srfA* operon (*srfAA*, *srfAB*, *srfAC*, *srfAD*) in microbes, which uses four amino acids (L-glutamate, L-leucine, L-valine, and L-aspartate) and fatty acids as precursors to form cyclic lipopeptide surfactin via a complex mechanism (condensation reaction) [34]. The biosynthesis pathway of surfactin was presented in Figure S4, which mainly contains three parts: the synthesis and activation of branched-chain fatty acids; the synthesis of the four amino acids; and the assembly of peptide chain. For surfactin, it can hardly achieve a significant breakthrough in production only through traditional fermentation optimization because of its low yield in wild strains [16, 35]. Strategies for surfactin overproduction were focused on strain modification recent

years, such as substitution of the native promoter P_{srf} of *srfA* operon [15, 16], overexpressing transporters to enhance surfactin efflux [18], and modifying the regulators ComX and PhrC [35]. However, most modifications were performed in existing strains. Engineering and modifying microbial chassis could maximize its practical application ranges and obtain maximum theoretical yields of bio-based products of interests. Such as *B. subtilis* BSK814, a genome-reduced strain, was endowed with the ability to hyperproduce guanosine as well as acetoin by modifying different metabolic pathways [4, 19].

In this study, the chassis GR167 harbored intact *srfA* operon and possessed superior industrially-relevant physiological traits, which was used as a starting strain to explore its ability of surfactin production. Because the fermentation broth incubated with NK-1 strain was too viscous to obtain a relatively purer surfactin product, the analysis of the production of surfactin by this strain and compared it with the yield observed for GR167 was difficult. For the γ-PGA-encoding gene *pgsBCA* was a main factor contributing to the high viscosity and the limitation of dissolved oxygen of the culture broth [36], consequently, a *pgsBCA*-deficient strain NK-ΔLP (NK-1 derivative, Δ*pgsBCA*) [37] was employed to as a control in the case of surfactin production. Surfactin production by GR167 and NK-ΔLP was demonstrated by high-performance liquid chromatography-mass spectrometry (HPLC-MS). A slight increase (approximately 9.7%) in the surfactin titer was observed with GR167 (Figure S2). The low difference in surafctin yield between the two strains may be mainly due to the deletion of *pgsBCA* in NK-ΔLP, because the surfactin biosynthesis-related genes of NK-ΔLP were up-regulated compared with that of *B. amyloliquefaciens* LL3 illustrated by transcriptome analysis (Figure S3). The genome reduction has little positive effect on the surfactin production, however, the chassis GR167 we constructed here possessed superior genetic operability (higher transformation efficiency). In addition, higher growth rate of GR167 was also a critical factor for ensuring that further metabolic modifications take place successfully. Consequently, it is interesting and necessary to explore whether microbial cell factories with high surfactin production capabilities can be constructed by further modification of GR167.

Characterization of surfactin produced by GR167

It was reported that surfactin produced by microorganisms is a mixture of several surfactin homologs [38]. In current study, by comparing the HPLC spectrogram of the produced surfactin by GR167 with that of the surfactin standard, there were four peaks be detected within a retention time of 6.4 min~7.2 min (Fig. 4a). To determine precisely the surfactin purity produced by GR167, each peak product of GR167 was purified from the culture supernatant and subjected to mass spectra (MS) analysis. The mass spectra of the peaks 1, 2, 3, and 4 products showing the molecular ion peaks at m/z 995, 1009, 1023, and 1037, which were attributed to $[C_{13} + 2H]^{2+}$, $[C_{14} + 2H]^{2+}$, $[C_{15} + 2H]^{2+}$, and $[C_{16} + 2H]^{2+}$, respectively (Figs. 4b and c). These compounds are surfactin homologs which differ in their β-hydroxy fatty acid chain length by 14 Da.

Enhancing surfactin production by blocking the potential competitive pathways

A transcriptional comparison between *B. amyloliquefaciens* LL3 and NK-ΔLP using RNA-seq revealed that the transcriptional levels of the gene clusters *srfA*, *itu* and *fen*, responsible for surfactin, iturin A and fengycin biosynthesis were all up-regulated when *pgsBCA* was removed (Figure S3). Iturin A and fengycin belonging to CLP antibiotics are structural analogues of surfactin [39], possibly leading to the reduction of the purity of the extracted surfactin from the culture supernatant. Iturin A and fengycin are synthesized by NRPSs like surfactin [13]; thus, they may share similar biosynthesis mechanisms with surfactin and their biosynthesis may compete for NADPH, energy and direct precursors with surfactin biosynthesis. In this study, the gene clusters *itu* (37.2 kb) and *fen* (11.5 kb) were deleted to enhance surfactin production. The resulting mutants were designated as GR167I (Δ*itu*), GR167D (Δ*fen*) and GR167ID (Δ*itu*, Δ*fen*). The titer of surfactin was increased to 32.88 mg/L in GR167ID, with a 10% and 56% improvement in the titer and specific productivity of surfactin compared to GR167, respectively (Figure S2). The synthesis pathway of surfactin indicated that blocking the potential competitive pathways can eliminate the competition for the same amino acid precursors, allowing for the redistribution of substrates and precursors towards surfactin biosynthesis (Figure S4).

Construction of endogenous promoter library of *B. amyloliquefaciens* LL3

Promoter engineering is considered as a promising approach for enhanced production of bacterial secondary metabolites [21, 22]. FPKM (fragments per kilobase million) value is positively correlated with the transcriptional activity of a gene [40], which therefore can be regarded as an indicator for initial screening of promoters. Through RNA-seq analysis of LL3, all genes were ranked and classified into three groups based on their FPKM values, i.e., lower than 1,250, 1,250-4,000 and higher than 4,000. Then, the first six genes with higher FPKM values in each group were selected, and their upstream regions were predicted and cloned as described in Methods, named PR_x [*x*: the name of various related genes; PR: the sequences of predicted promoters with their ribosomal binding sites (RBSs)] and represented weak, moderate and strong promoters, respectively (Table S3). Subsequently, various reporter gene vectors derived from pHT01 containing fused fragments of the predicted promoters and *gfp* gene were used to assess the strengths of the tested promoters in LL3 (Figure S5).

Characterization of the selected promoters via RT-qPCR and GFP fluorescence measurement

As shown in Fig. 5a, the relative transcriptional levels of the candidate promoters measured with reporter gene vectors were PR_{ldh}, PR_{ahp}, PR_{hem}, PR_{tpxi}, PR_{clp}, PR_{suc}, PR_{accD}, PR_{gltA}, PR_{rpsu}, PR_{nfrA}, PR_{gltX}, PR_{ydh}, PR_{ugt}, PR_{arg}, PR_{nad}, PR_{lac}, PR_{alsD}, PR_{hom} and PR_{pgmi} in a descending order, which were inconsistent with the strengths of the promoters shown by the FPKM values (Table S3), with similar results reported in a previous study [23]. We speculate that the transcription of a gene on chromosome may be affected and

regulated by flanking genes and regulatory sequences. However, this interference could be eliminated if a promoter is inserted into a plasmid.

To better evaluate these endogenous promoters, the relative fluorescence intensities of GFP was measured. Among the 18 endogenous promoters, PR_{ahp}, PR_{suc} and PR_{tpxi} showed superior production capacity of GFP, followed by PR_{rpsU}, PR_{hem} and PR_{ydh} (Fig. 5b). However, the first six promoters were PR_{ldh}, PR_{ahp}, PR_{hem}, PR_{tpxi}, PR_{clp} and PR_{suc} from high to low at the transcriptional levels (Fig. 5a). The different RBSs located upstream of the promoters may affect the translational initiation efficiencies of mRNA corresponding to GFP, leading to the different trends between the transcriptional level and production capacity of GFP.

Substitution of the native *srfA* promoter further enhanced surfactin production

Considering the heterologous expression of *srfA* is challenging for which large genetic sequence (over 25 kb), substitution of the native *srfA* promoter by strong promoters is considered more beneficial for enhanced transcription of *srfA* operon [15, 16, 20]. In this study, two promoters PR_{suc} and PR_{tpx} with better transcription and expression levels were integrated into upstream of the *srfA* operon in GR167ID, generating mutant strains GR167IDS and GR167IDT, respectively. The nucleotide sequences of the two selected promoters are shown in supplementary material. As expected, both the surfactin production and specific productivity exhibited a significant elevation (Figs. 6a and b). In particular, the PR_{suc} promoter-substituted strain GR167IDS produced 311.35 mg/L surfactin, which was about 9.5-fold higher than that of GR167ID (Fig. 6a). Meanwhile, the transcriptional level of *srfA* in GR167IDS was 678-fold higher than that in GR167ID (Fig. 6c), melting curves of *srfA* and its internal standard gene *rpsU* showed that there are no non-specific products (Figure S6).

Since the replacement of *srfA* promoter with PR_{suc} promoter significantly increased the surfactin titer compared with other modifications (genome reduction and blocking of competitive pathways). We further modified NK-ΔLP with PR_{suc} promoter substitution to generate mutant strain ΔLPS, while, whose surfactin production was approximately 1.7-fold lower than that of GR167IDS. Vlamakis et al. point out that extracellular polysaccharides could form biofilm stimulated by surfactin and which synthesis was accompanied by large number of substrates and energy consumption [41]. Sufficient supply of precursors and energy is an indispensable factor for the large-scale synthesis of products. Genomic information shows that the final hyperproducer GR167IDS removed not only the biosynthesis of extracellular polysaccharides (Table S2, deleted region of G1) and other compounds (iturin, fengycin, γ-PGA, and bacillaene) that compete with surfactin for the same precursors (i.e., glutamate/glutamine and acetyl-coA) (Figure S4; Table S2), but also large amounts of hypothetical proteins, which functions and interaction with other genes or regulatory factors in the cytoplasm are unknown. Thus, the reduced genome may contribute to the improvement of overall cellular metabolic activity, and the high performance of GR167IDS in surfactin production should be the synergistic effect of all these factors.

Conclusions

In summary, a genome-reduced strain GR167 was constructed by deleting some non-essential genes accounting for ~ 4.18% of the LL3 genome and outcompeted the parental strain in several physiological traits assessed. GR167IDS, obtained from GR167 by promoter substitution, showed a 10.4-fold improvement in the titer of surfactin compared to GR167. The current results suggest that genome reduction in combination with promoter engineering may be a feasible strategy for the development of microbial cell factories capable of efficiently producing bacterial secondary metabolites.

Methods

Bacterial strains, media, and culture conditions

Escherichia coli DH5α was employed for plasmid construction and propagation. For the subsequent successful electroporation of *B. amyloliquefaciens* strains, the *E. coli* JM110 was used as intermediate host to demethylate the desirable plasmids from *E. coli* DH5α. *E. coli* strains were incubated at 37 °C in Luria–Bertani (LB) broth. *B. amyloliquefaciens* LL3 was deposited in the China Center for Type Culture Collection (CCTCC) (accession number: CCTCC M 208109). *B. amyloliquefaciens* NK-1 was employed as the parental strain for genome reduction. GR167 was used as the starting strain for engineered high-yielding surfactin producing mutants. M9 medium, which contains 3.4 g/L $Na_2HPO{\cdot}12H_2O$, 0.6 g/L KH_2PO_4 0.1 g/L NaCl 0.2 g/L NH_4Cl supplemented with 20 g/L glucose, 50 mg/L tryptophan and 200 mM MOPS, was used for assessing growth of relevant strains. For lipopeptide surfactin production, *B. amyloliquefaciens* was incubated at 30 °C and 180 rpm for 48 h in Landy medium [42]. When appropriate, media were supplemented with ampicillin (Ap; 100 μg/mL), chloramphenicol (Cm; 5 μg/mL) or 5-fluorouracil (5-FU; 1.3 mM).

Plasmid and strain construction

To construct the gene deletion vectors, the temperature-sensitive plasmid pKSU with an *upp* expression cassette was used [25]. The upstream and downstream fragments of the deleted genomic regions were amplified by PCR and then the two fragments were joined by overlap PCR. The generated fragment was ligated into pKSU via homologous recombination, to generate the gene deletion vectors. Introduction of plasmid into *B. amyloliquefaciens* was carried out using an optimized high osmolarity electroporation method [36]. To carry out multiple gene deletions on a single strain, a marker-less gene deletion method was used to construct the gene knockout mutants [24]. All the constructed plasmids and mutant strains were validated by PCR detection and DNA sequencing. All plasmids, strains, and primers used in this study are listed in Table S4, Table 2, and Table S5, respectively.

Physiological traits assessment

Growth profiles of GR167 and NK-1 were measured in both M9 mineral medium and LB medium. Overnight cultures (1 mL) were inoculated into 100 mL LB or M9 medium in 500-mL flasks and then incubated for 20 h at 37 °C and 180 rpm. To determine the bacterial growth status, the OD_{600} was monitored every 2 h using a UV-1800 spectrophotometer (Shimadzu, Kyoto, Japan).

The metabolic phenotypic analyses were performed with a Biolog GEN Ш MicroPlate™ using a phenotype microarray system (Biolog Inc., California, USA) according to the manufacturer's instructions. The bacterial cells on the solid medium surface were collected by cotton swab, dissolved into the inoculating fluid IF-B, and then the cell density was adjusted to a range of 80-86% Turbidity. Subsequently, 100 µl of bacterial suspensions were pipetted into the Biolog GEN Ш plates with different substrates. After the samples were incubated at 33 °C for 48 h, the absorbance at 590 nm was measured with the Biolog reader and the test data were analyzed by the Biolog system.

Electro-competent cells of GR167 and NK-1 (2×10^{10} CFU/mL) were prepared according to previous methods [36]. Subsequently, approximately 100 ng of plasmid pHT01 was absorbed by 100 µL of electro-competent cells via electroporation. After 3 h of recover at 37 °C and 180 rpm, the mixture was spread on LB agar plates supplemented with 5 µg/mL Cm. The numbers of colonies were calculated to evaluate the transformation efficiency.

Cells were cultured in LB medium at 37 °C for 18 h. The intracellular cofactors NADPH and $NADP^+$ were extracted and quantified by enzymatic methods [42] using an EnzyChrom™ assay kit (BioAssay Systems, USA) according to the manufacturer's protocols.

The heterologous protein productivity was determined by introducing plasmid pHT-P_{43}-*gfp* into GR167 and NK-1. The detailed protocols for strain cultivation and fluorescence intensity measurement refer to our previous work [9]. The relative fluorescence intensity was normalized against per OD_{600} of whole cells. The fluorescence signal of NK-1 harboring pHT01 was set as background and was subtracted from overall fluorescence.

RNA-seq, promoter prediction, and construction of reporter gene vectors

RNA-seq analyses of LL3 were carried out according to our previous methods [32]. The expression levels of the predicted genes were quantified as the FPKM value [43]. The upstream regions of genes with different FPKM values were submitted online (http://www.fruitfly.org/seq_tools/promoter) for promoter prediction.

Furthermore, each promoter sequence plus its native RBS and *gfp* gene were amplified by PCR from the LL3 genome and pHT-P_{43}-*gfp*, respectively. Subsequently, 3'-end of a promoter sequence was fused with

5'-end of *gfp* gene and the fusion fragment was inserted into plasmid pHT01, to generate reporter gene vector pHT-PR_X-*gfp* for promoter strength characterization (Figure S5). Moreover, a control vector pHT-PR_{lac}-*gfp* with *gfp* expression driven by *lac* promoter was similarly constructed with pHT01.

Total RNA extraction, qPCR analyses, and GFP fluorescence measurement of reporter gene vectors

An appropriate number of cells from LB or Landy cultures were collected to isolate total RNA with the RNApure Bacteria kit (DNase I) (Cwbio, Beijing, China). Afterwards, complementary DNA (cDNA) was prepared with approximately 0.5 μg total RNA as template employing the HiScript® II Q RT SuperMix (Vazyme). To determine the transcriptional strength of relevant genes, qPCR analysis was carried out with ChamQ Universal SYBR qPCR Master Mix (Vazyme) and cDNA as the template. The relative gene transcription levels were calculated against that of *rpsU* gene as the internal standard using the $2^{-\Delta\Delta Ct}$ method [44, 45]. The relative transcriptional activity of a promoter was normalized against that of *lac* promoter. In addition, GFP fluorescence measurement was performed as described previously [9].

Surfactin isolation and HPLC-MS analyses

All tested strains were cultured aerobically at 180 rpm in the Landy medium for 48 h. The culture supernatant and bacterial cell were separated by centrifugation at 4 °C and 14,000 rpm for 20 min. Subsequently, the bacterial cell was lyophilized for 24 h and weighed to obtain the cell dry weight (CDW). The supernatant was acidified to pH 2.0 with 6 M HCl and precipitated overnight at 4 °C. The precipitate formed was harvested by centrifugation and resuspended with 100 mL methyl alcohol. After which, 1 M NaOH was added to adjust the pH to 7.0 and further incubated for 48 h at 180 rpm and 37 °C. The supernatant containing surfactin extract was collected by centrifugation. The recovery and purification of surfactin homologues referred to the previous method [17]. Prior to HPLC-MS analysis, the supernatant was concentrated through a vacuum rotary evaporator and filtered via a 0.22-μm filter. Surfactin was analyzed and quantified by HPLC-MS equipped with a C18 column (Innoval ODS-2, 250 mm × 4.6 mm × 5 μm, Phenomenex, USA) using a validated method described previously [17, 43]. The extracted surfactin samples (20 μL) were injected into the HPLC-MS system with a mobile phase consisting of acetonitrile and water (55:45, v/v) at a flow rate of 0.8 mL/min. Surfactin was detected at 210 nm.

Declarations

Funding

This work was supported by the National Key Research and Development Program of China (2018YFA0900100), the National Natural Science Funding of China (31670093) and the Tianjin Natural

Science Funding (18JCYBJC24500).

Acknowledgements

All of the authors thank the editor and the anonymous reviewers for their valuable comments.

Authors' contributions

FZ and CY designed this study. FZ, KYH, YFQ and WXG performed these experiments. FZ, KYH, XYS, WXG and SFW carried out the data analysis. FZ and CY wrote the manuscript.

Availability of date and materials

All data generated or analyzed during the current study are included in this published article and its supplementary material.

Ethics approval and consent to participate

Not applicable.

Consent for publication

Not applicable.

Competing interests

The authors declare that they have no competing interests.

References

1. Koonin EV: Comparative genomics, minimal gene-sets and the last universal common ancestor. Nat Rev Microbiol 2003;1:127-136.
2. Juhas M, Reuß DR, Zhu B, Commichau FM: *Bacillus subtilis* and *Escherichia coli* essential genes and minimal cell factories after one decade of genome engineering. Microbiology 2014;160:2341-2351.

3. Leprince A, van Passel MW, dos Santos VA: Streamlining genomes: toward the generation of simplified and stabilized microbial systems. Curr Opin Biotechnol 2012;23:651-658.
4. Li Y, Zhu X, Zhang X, Fu J, Wang Z, Chen T, Zhao X: Characterization of genome-reduced *Bacillus subtilis* strains and their application for the production of guanosine and thymidine. Microb Cell Fact 2016;15:94.
5. Zhu D, Fu Y, Liu F, Xu H, Saris PE, Qiao M: Enhanced heterologous protein productivity by genome reduction in *Lactococcus lactis* NZ9000. Microb Cell Fact 2017;16:1.
6. Mizoguchi H, Sawano Y, Kato J, Mori H: Superpositioning of deletions promotes growth of *Escherichia coli* with a reduced genome. DNA Res 2008;15:277-284.;
7. Morimoto T, Kadoya R, Endo K, Tohata M, Sawada K, Liu S, Ozawa T, Kodama T, Kakeshita H, Kageyama Y, et al: Enhanced recombinant protein productivity by genome reduction in *Bacillus subtilis*. DNA Res 2008; 15:73-81.
8. Aguilar Suárez R, Stülke J, van Dijl JM: **Less Is More:** Toward a Genome-Reduced *Bacillus* Cell Factory for "Difficult Proteins". ACS Synth Biol 2019;8:99-108.
9. Liang P, Zhang Y, Xu B, Zhao Y, Liu X, Gao W, Ma T, Yang C, Wang S, Liu R: Deletion of genomic islands in the *Pseudomonas putida* KT2440 genome can create an optimal chassis for synthetic biology applications. *Microb Cell Fact* 2020;19:70.
10. Hu F, Liu Y, Li S: Rational strain improvement for surfactin production: enhancing the yield and generating novel structures. Microb Cell Fact 2019;18:42.
11. Wu Q, Zhi Y, Xu Y: Systematically engineering the biosynthesis of a green biosurfactant surfactin by *Bacillus subtilis* 168. Metab Eng 2019;52:87-97.
12. Deravel J, Lemière S, Coutte F, Krier F, Van Hese N, Béchet M, Sourdeau N, Höfte M, Leprêtre A, Jacques P: Mycosubtilin and surfactin are efficient, low ecotoxicity molecules for the biocontrol of lettuce downy mildew. Appl Microbiol Biotechnol 2014;98:6255-6264.
13. Seydlová G, Svobodová JJCEJoM: Review of surfactin chemical properties and the potential biomedical applications. 2008;3:123-133.
14. Lai CC, Huang YC, Wei YH, Chang JS: Biosurfactant-enhanced removal of total petroleum hydrocarbons from contaminated soil. J Hazard Mater 2009;167:609-614.
15. Sun H, Bie X, Lu F, Lu Y, Wu Y, Lu Z: Enhancement of surfactin production of *Bacillus subtilis* fmbR by replacement of the native promoter with the Pspac promoter. Can J Microbiol 2009;55:1003-1006.
16. Jiao S, Li X, Yu H, Yang H, Li X, Shen Z: In situ enhancement of surfactin biosynthesis in *Bacillus subtilis* using novel artificial inducible promoters. Biotechnol Bioeng 2017;114:832-842.
17. Dang Y, Zhao F, Liu X, Fan X, Huang R, Gao W, Wang S, Yang C: Enhanced production of antifungal lipopeptide iturin A by *Bacillus amyloliquefaciens* LL3 through metabolic engineering and culture conditions optimization. Microb Cell Fact 2019;18:68.
18. Li X, Yang H, Zhang D, Li X, Yu H, Shen Z: Overexpression of specific proton motive force-dependent transporters facilitate the export of surfactin in *Bacillus subtilis*. J Ind Microbiol Biotechnol

2015;42:93-103.

19. Yan P, Wu Y, Yang L, Wang Z, Chen T: Engineering genome-reduced *Bacillus subtilis* for acetoin production from xylose. Biotechnol Lett 2018;40:393-398.
20. Willenbacher J, Mohr T, Henkel M, Gebhard S, Mascher T, Syldatk C, Hausmann R: Substitution of the native srfA promoter by constitutive Pveg in two *B. subtilis* strains and evaluation of the effect on Surfactin production. J Biotechnol 2016;224:14-17.
21. Zhao F, Liu X, Kong A, Zhao Y, Fan X, Ma T, Gao W, Wang S, Yang C: Screening of endogenous strong promoters for enhanced production of medium-chain-length polyhydroxyalkanoates in *Pseudomonas mendocina* NK-01. Sci Rep 2019;9:1798.
22. Luo Y, Zhang L, Barton KW, Zhao H: Systematic Identification of a Panel of Strong Constitutive Promoters from *Streptomyces albus*. ACS Synth Biol 2015;4:1001-1010.
23. Geng W, Cao M, Song C, Xie H, Liu L, Yang C, Feng J, Zhang W, Jin Y, Du Y, Wang S: Complete genome sequence of *Bacillus amyloliquefaciens* LL3, which exhibits glutamic acid-independent production of poly-γ-glutamic acid. J Bacteriol 2011;193:3393-3394.
24. Zhang W, Gao W, Feng J, Zhang C, He Y, Cao M, Li Q, Sun Y, Yang C, Song C, Wang S: A markerless gene replacement method for *B. amyloliquefaciens* LL3 and its use in genome reduction and improvement of poly-γ-glutamic acid production. Appl Microbiol Biotechnol 2014;98:8963-8973.
25. Feng J, Gao W, Gu Y, Zhang W, Cao M, Song C, Zhang P, Sun M, Yang C, Wang S: Functions of poly-gamma-glutamic acid (γ-PGA) degradation genes in γ-PGA synthesis and cell morphology maintenance. Appl Microbiol Biotechnol 2014;98:6397-6407.
26. Vernikos GS, Parkhill J: Resolving the structural features of genomic islands: a machine learning approach. Genome Res 2008;18:331-342.
27. Jani M, Sengupta S, Hu K, Azad RK: Deciphering pathogenicity and antibiotic resistance islands in methicillin-resistant *Staphylococcus aureus* genomes. Open Biol 2017;7.
28. Kolisnychenko V, Plunkett G, 3rd, Herring CD, Fehér T, Pósfai J, Blattner FR, Pósfai G: Engineering a reduced *Escherichia coli* genome. Genome Res 2002;12:640-647.
29. Kurokawa M, Seno S, Matsuda H, Ying BW: Correlation between genome reduction and bacterial growth. DNA Res 2016;23:517-525.
30. Hamoen LW, Venema G, Kuipers OP: Controlling competence in *Bacillus subtilis*: shared use of regulators. Microbiology 2003;149:9-17.
31. Martínez I, Zhu J, Lin H, Bennett GN, San KY: Replacing *Escherichia coli* NAD-dependent glyceraldehyde 3-phosphate dehydrogenase (GAPDH) with a NADP-dependent enzyme from *Clostridium acetobutylicum* facilitates NADPH dependent pathways. Metab Eng 2008;10:352-359.
32. Feng J, Quan Y, Gu Y, Liu F, Huang X, Shen H, Dang Y, Cao M, Gao W, Lu X, et al: Enhancing poly-γ-glutamic acid production in *Bacillus amyloliquefaciens* by introducing the glutamate synthesis features from Corynebacterium glutamicum. Microb Cell Fact 2017;16:88.

33. Lieder S, Nikel PI, de Lorenzo V, Takors R: Genome reduction boosts heterologous gene expression in *Pseudomonas putida*. Microb Cell Fact 2015;14:23.
34. Wang C, Cao Y, Wang Y, Sun L, Song H: Enhancing surfactin production by using systematic CRISPRi repression to screen amino acid biosynthesis genes in *Bacillus subtilis*. Microb Cell Fact 2019;18:90.
35. Jung J, Yu KO, Ramzi AB, Choe SH, Kim SW, Han SO: Improvement of surfactin production in *Bacillus subtilis* using synthetic wastewater by overexpression of specific extracellular signaling peptides, comX and phrC. Biotechnol Bioeng 2012;109:2349-2356.
36. Zhang W, Xie H, He Y, Feng J, Gao W, Gu Y, Wang S, Song C: Chromosome integration of the Vitreoscilla hemoglobin gene (vgb) mediated by temperature-sensitive plasmid enhances γ-PGA production in *Bacillus amyloliquefaciens*. FEMS Microbiol Lett 2013;343:127-134.
37. Feng J, Gu Y, Han L, Bi K, Quan Y, Yang C, Zhang W, Cao M, Wang S, Gao W, et al: Construction of a *Bacillus amyloliquefaciens* strain for high purity levan production. FEMS Microbiol Lett 2015;362.
38. Yang H, Li X, Li X, Yu H, Shen Z: Identification of lipopeptide isoforms by MALDI-TOF-MS/MS based on the simultaneous purification of iturin, fengycin, and surfactin by RP-HPLC. Anal Bioanal Chem 2015;407:2529-2542.
39. Zhao H, Shao D, Jiang C, Shi J, Li Q, Huang Q, Rajoka MSR, Yang H, Jin M: Biological activity of lipopeptides from *Bacillus.* Appl Microbiol Biotechnol 2017;101:5951-5960.
40. Mortazavi A, Williams BA, McCue K, Schaeffer L, Wold B: Mapping and quantifying mammalian transcriptomes by RNA-Seq. Nat Methods 2008;5:621-628.
41. Vlamakis H, Chai Y, Beauregard P, Losick R, Kolter R: Sticking together: building a biofilm the *Bacillus subtilis* way. Nat Rev Microbiol 2013;11:157-168.
42. Bergmeyer HU, Bergmeyer J, Graßl M: Methods of enzymatic analysis. Verlag Chemie;1984.
43. Gao W, Liu F, Zhang W, Quan Y, Dang Y, Feng J, Gu Y, Wang S, Song C, Yang C: Mutations in genes encoding antibiotic substances increase the synthesis of poly-γ-glutamic acid in *Bacillus amyloliquefaciens* LL3. Microbiologyopen 2017;6.
44. Reiter L, Kolstø AB, Piehler AP: Reference genes for quantitative, reverse-transcription PCR in *Bacillus cereus* group strains throughout the bacterial life cycle. J Microbiol Methods 2011;86:210-217.
45. Livak KJ, Schmittgen TD: Analysis of relative gene expression data using real-time quantitative PCR and the 2(-Delta Delta C(T)) Method. Methods 2001;25:402-408.
46. Feng J, Gu Y, Wang J, Song C, Yang C, Xie H, Zhang W, Wang S: Curing the plasmid pMC1 from the poly (γ-glutamic acid) producing *Bacillus amyloliquefaciens* LL3 strain using plasmid incompatibility. Appl Biochem Biotechnol 2013;171:532-542.

Tables

Table 1 Metabolic phenotype analysis of NK-1 and GR167

Substrate	NK-1	GR167
Methyl Pyruvate	94	118
L-Aspartic Acid	178	232
Tween 40	77	79
D-Lactic Acid Methyl Ester	61	67
Citric Acid	245	254
L-Malic Acid	227	241
Formic Acid	90	105
Acetic Acid	82	87
D-Sorbitol	129	94
D-Maltose	138	106
D-Trehalose	198	154
D-Cellobiose	195	146
Gentiobiose	84	78
Sucrose	191	155
α-D- Lactose	140	113
α-D- Glucose	208	161
D- Mannose	185	146
D- Fructose	74	83
Glycerol	255	174
L-Glutamic Acid	229	231
L-Lactic Acid	191	193
γ-Amino-Butryric Acid	144	113
Acetoacetic Acid	112	108

Table 2 Strains used in this study

Strains	Relative characteristics	source
B. amyloliquefaciens		
GR01	LL3 derivative, Δ*upp*	[24]
GR07 (NK-1)	GR01 ΔG0, 0.18% reduction of genome	[46]
GR22	GR07 ΔG1, 0.55% reduction of genome	This work
GR46	GR22 ΔG2, 1.15% reduction of genome	This work
GR94	GR46 ΔG3, 2.36% reduction of genome	This work
GR134	GR94 ΔG4, 3.36% reduction of genome	This work
GR164	GR134 ΔG5, 4.11% reduction of genome	This work
GR167	GR164 ΔG6, 4.18% reduction of genome	This work
NK-ΔLP	NK-1 derivative, Δ*pgsBCA*	[37]
GR167I	GR167 derivative, Δ*itu* cluster	This work
GR167D	GR167 derivative, Δ*fen* cluster	This work
GR167ID	GR167 derivative, Δ*itu* Δ*fen* clusters	This work
LL3-PR_{lac}	LL3 derivative, containing plasmid pHT-PR_{lac}-*gfp*	This work
LL3-PR_{ugt}	LL3 derivative, containing plasmid pHT-PR_{ugt}-*gfp*	This work
LL3-PR_{suc}	LL3 derivative, containing plasmid pHT-PR_{suc}-*gfp*	This work
LL3-PR_{ydh}	LL3 derivative, containing plasmid pHT-PR_{ydh}-*gfp*	This work
LL3-PR_{accD}	LL3 derivative, containing plasmid pHT-PR_{accD}-*gfp*	This work
LL3-PR_{clp}	LL3 derivative, containing plasmid pHT-PR_{clp}-*gfp*	This work
LL3-PR_{tpxi}	LL3 derivative, containing plasmid pHT-PR_{tpxi}-*gfp*	This work
LL3-PR_{gltX}	LL3 derivative, containing plasmid pHT-PR_{gltX}-*gfp*	This work
LL3-PR_{nad}	LL3 derivative, containing plasmid pHT-PR_{nad}-*gfp*	This work
LL3-PR_{arg}	LL3 derivative, containing plasmid pHT-PR_{arg}-*gfp*	This work
LL3-PR_{gltA}	LL3 derivative, containing plasmid pHT-PR_{gltA}-*gfp*	This work
LL3-PR_{ahp}	LL3 derivative, containing plasmid pHT-PR_{ahp}-*gfp*	This work
LL3-PR_{nrfA}	LL3 derivative, containing plasmid pHT-PR_{nrfA}-*gfp*	This work
LL3-PR_{pgmi}	LL3 derivative, containing plasmid pHT-PR_{pgmi}-*gfp*	This work
LL3-PR_{hom}	LL3 derivative, containing plasmid pHT-PR_{hom}-*gfp*	This work
LL3-PR_{hem}	LL3 derivative, containing plasmid pHT-PR_{hem}-*gfp*	This work
LL3-PR_{ldh}	LL3 derivative, containing plasmid pHT-PR_{ldh}-*gfp*	This work
LL3-PR_{rpsU}	LL3 derivative, containing plasmid pHT-PR_{rpsU}-*gfp*	This work
LL3-PR_{alsD}	LL3 derivative, containing plasmid pHT-PR_{alsD}-*gfp*	This work
GR167IDS	GR167ID derivative with its native *srf* promoter replaced by PR_{suc} promoter	This work
GR167IDT	GR167ID derivative with its native *srf* promoter replaced by PR_{tpxi} promoter	This work
E. coli strains		
DH5α	*supE44* Δ*lacU169*(_*80 lacZ*ΔM15) *recA1 endA1 hsdR17*(r_K^- m_K^+) *thi-1gyrA relA1* F^- Δ(*lacZYA-argF*)	Transgene
JM110	F^-*dam*-13::Tn9 (Cam^r) *dcm*-6 *hsdR2* ($r_k^-m_k^+$) *leuB6 hisG4 thi-1 araC14 lacY1 galK2 galT22 xylA5 mtl-1 rpsL136* (Str^r) *fhuA31 tsx-8 glnV*44 *mcrA mcrB*1	Fermentas

Figures

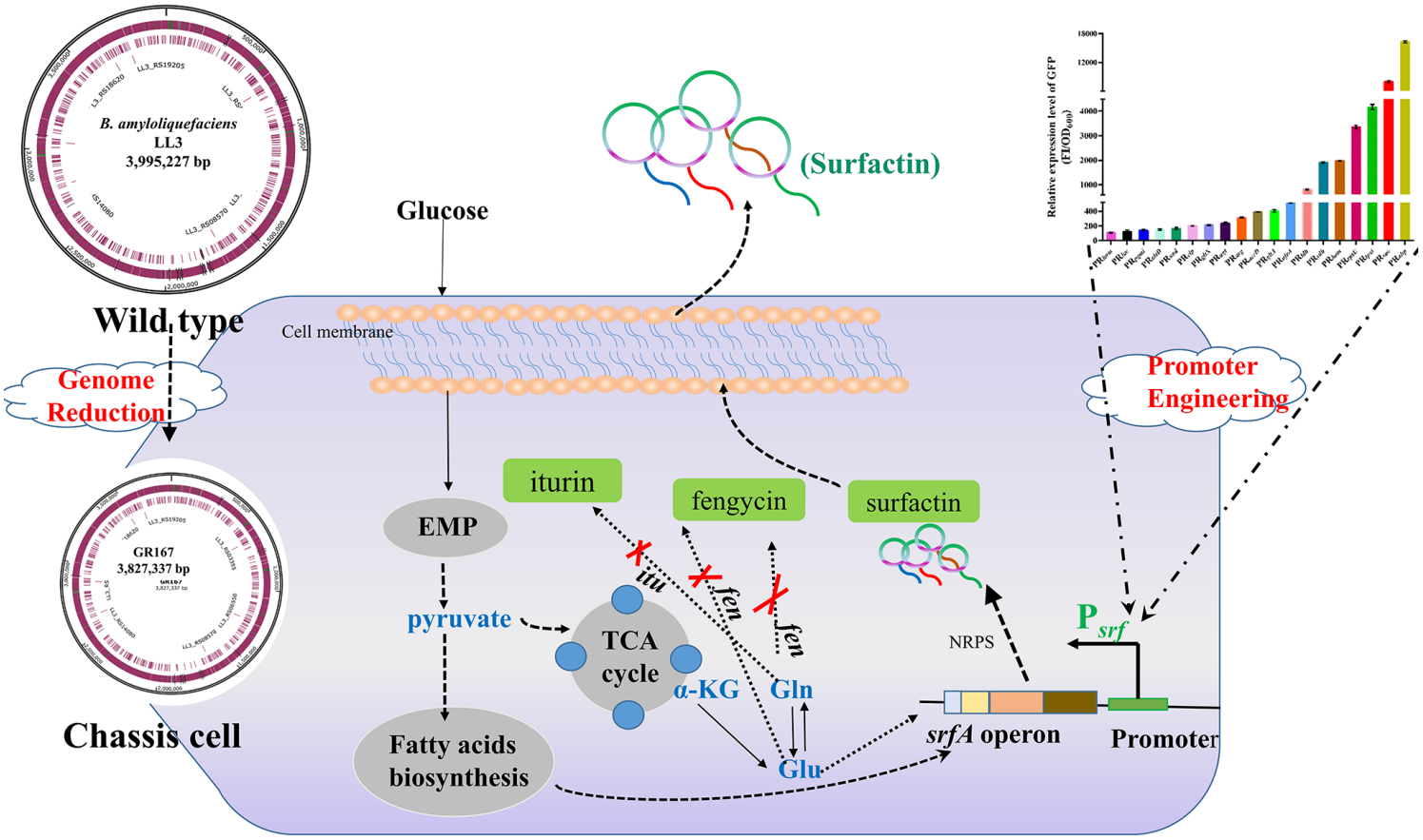

Figure 1

Schematic diagram of the overall strategy for enhancing lipopeptide surfactin yield in B. amyloliquefaciens.

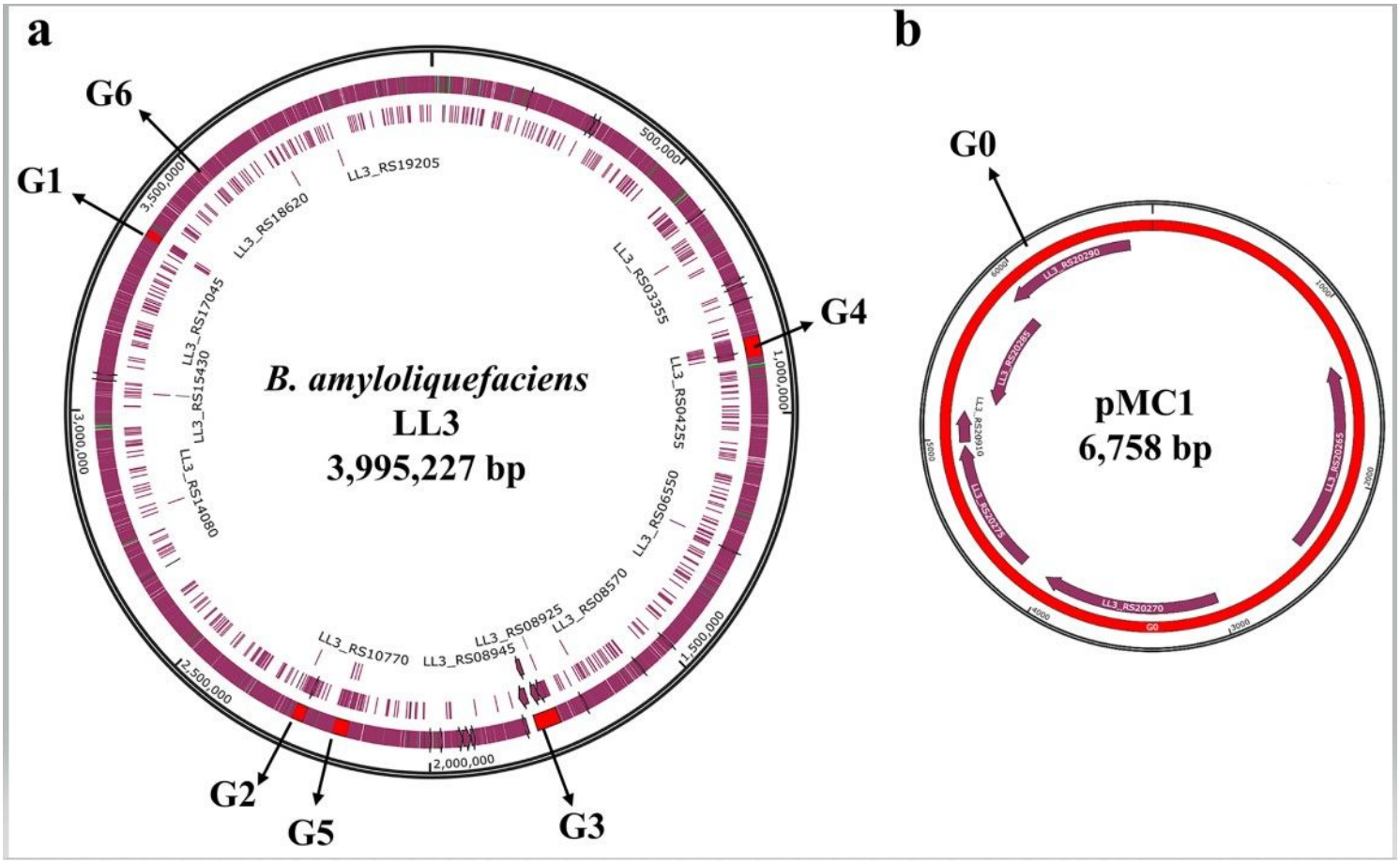

Figure 2

The construction of genome-reduced strain GR167. a The exact coordinates of the deleted regions (G1 to G6) on the chromosome of B. amyloliquefaciens LL3; b the physical map of the cured endogenous plasmid pMC1

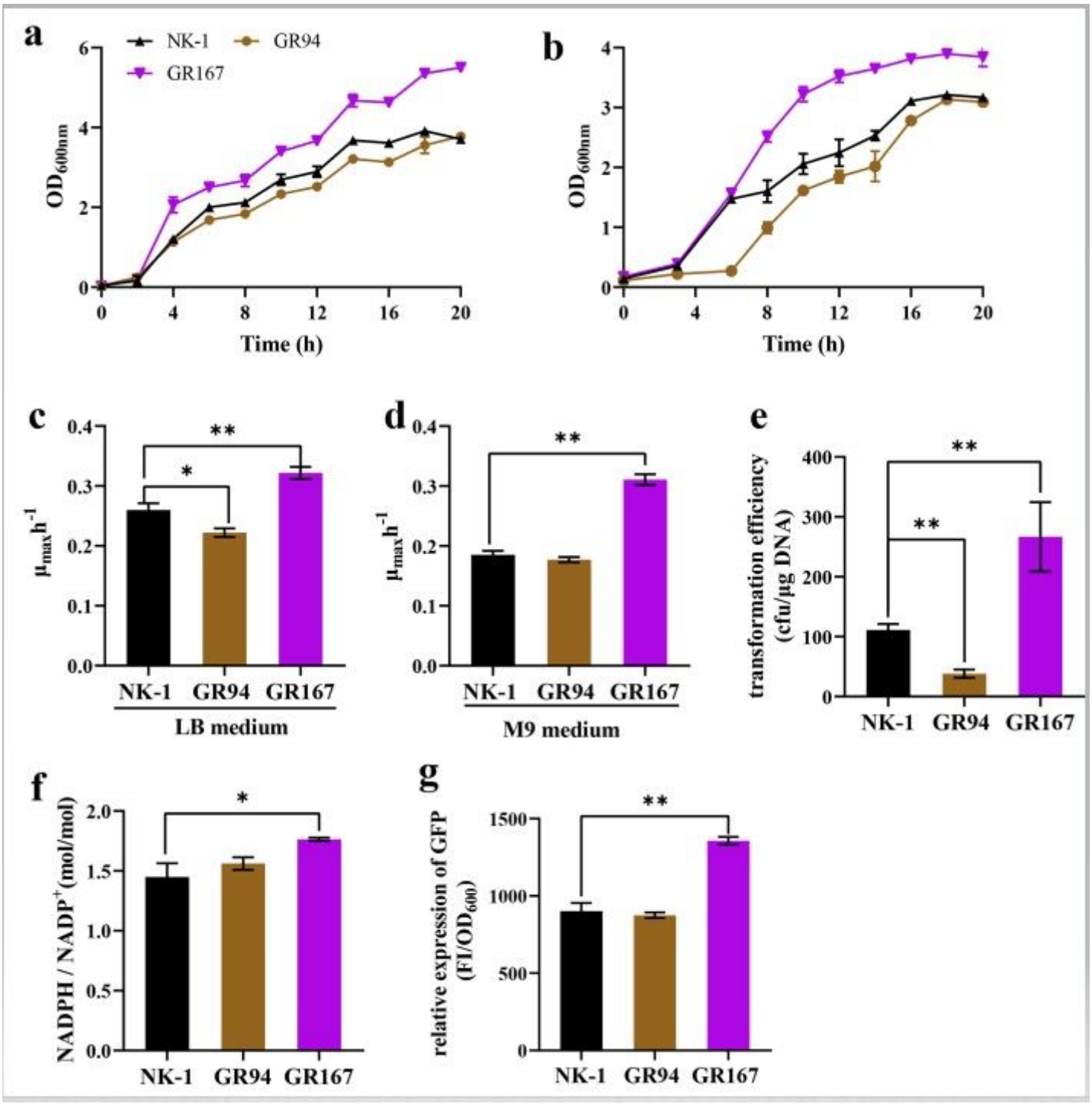

Figure 3

Physiological characteristics assessment of strains. a Growth curves measured in LB medium; b growth curves measured in M9 medium; c the maximum specific growth rate (μmax) measured in LB medium; d the μmax measured in M9 medium; e transformation efficiency; f intracellular reducing power level (NADPH/NADP+ molar ratio); g The relative fluorescence intensities (GFP, green fluorescent protein; FI, fluorescence intensity). Values denote mean ± SD of triplicates (*P < 0.05, **P < 0.01)

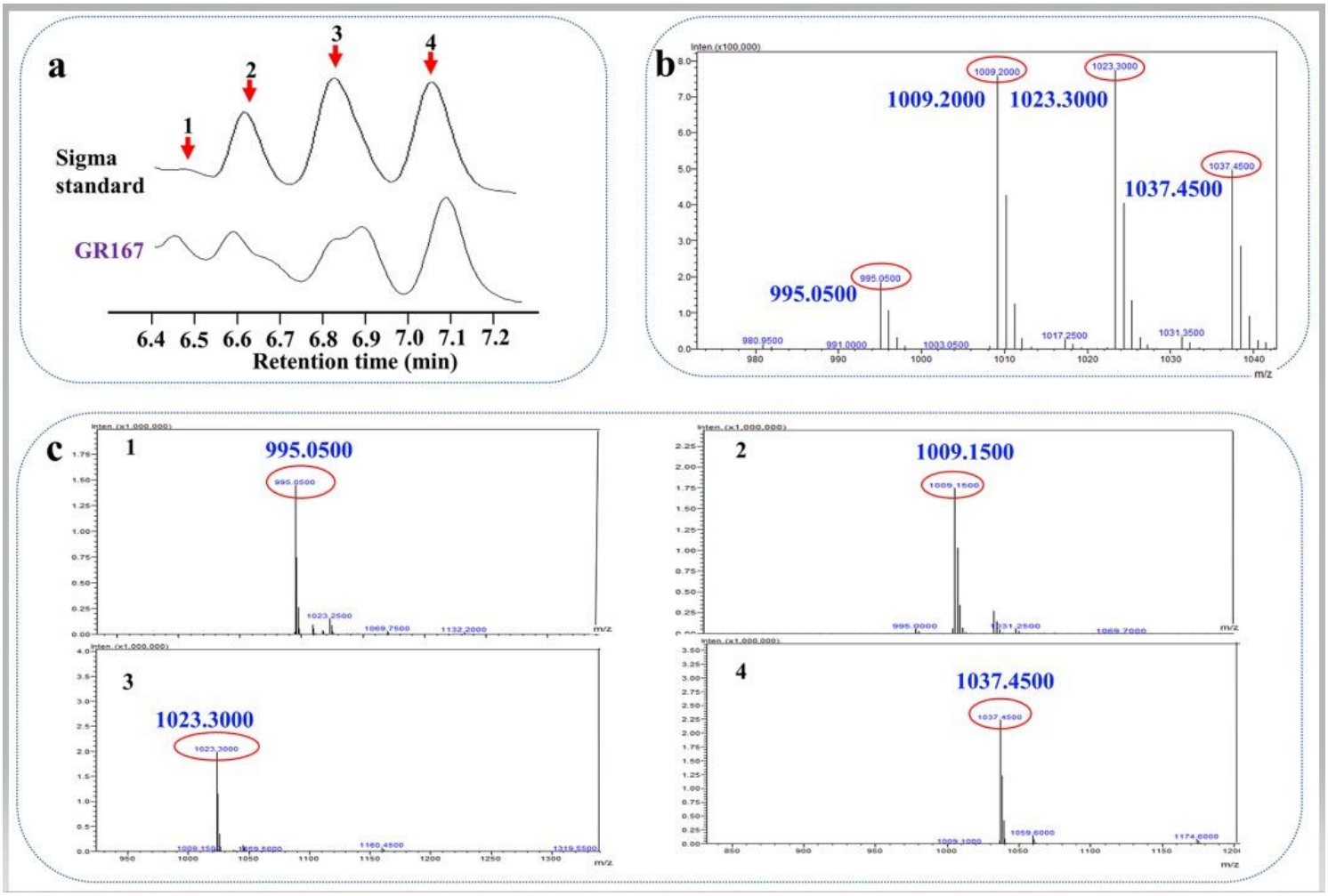

Figure 4

HPLC-MS chromatograms of surfactin standard and the samples produced by GR167. a HPLC chromatograms of surfactin from standard and GR167; b MS (mass spectra) of surfactin standard (Sigma); c MS of purified surfactin homologs produced by GR167. The peaks 1, 2, 3, and 4 products corresponding to the molecular ion peaks at m/z 995, 1009, 1023, and 1037, respectively

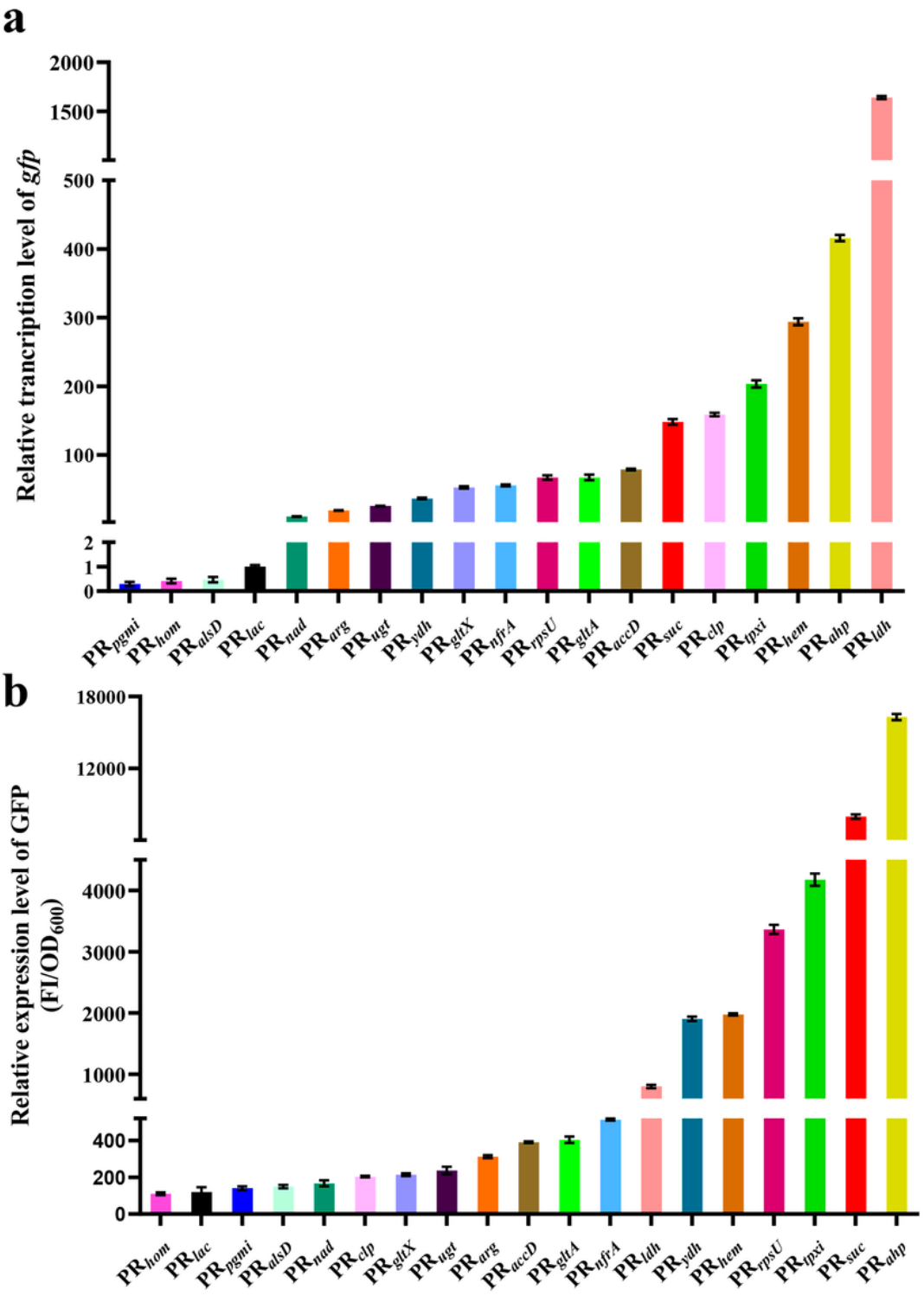

Figure 5

Characterization of the strengths of the selected endogenous promoters using reporter gene assays in LL3. a Transcriptional levels of gfp gene quantified via qPCR under the control of different promoters (rpsU gene was used as internal standard; the transcriptional level of gfp gene controlled by lac promoter was set as 1); b the relative fluorescence intensity of GFP (FI/OD600) under the control of different promoters. Values denote mean ± SD of triplicates

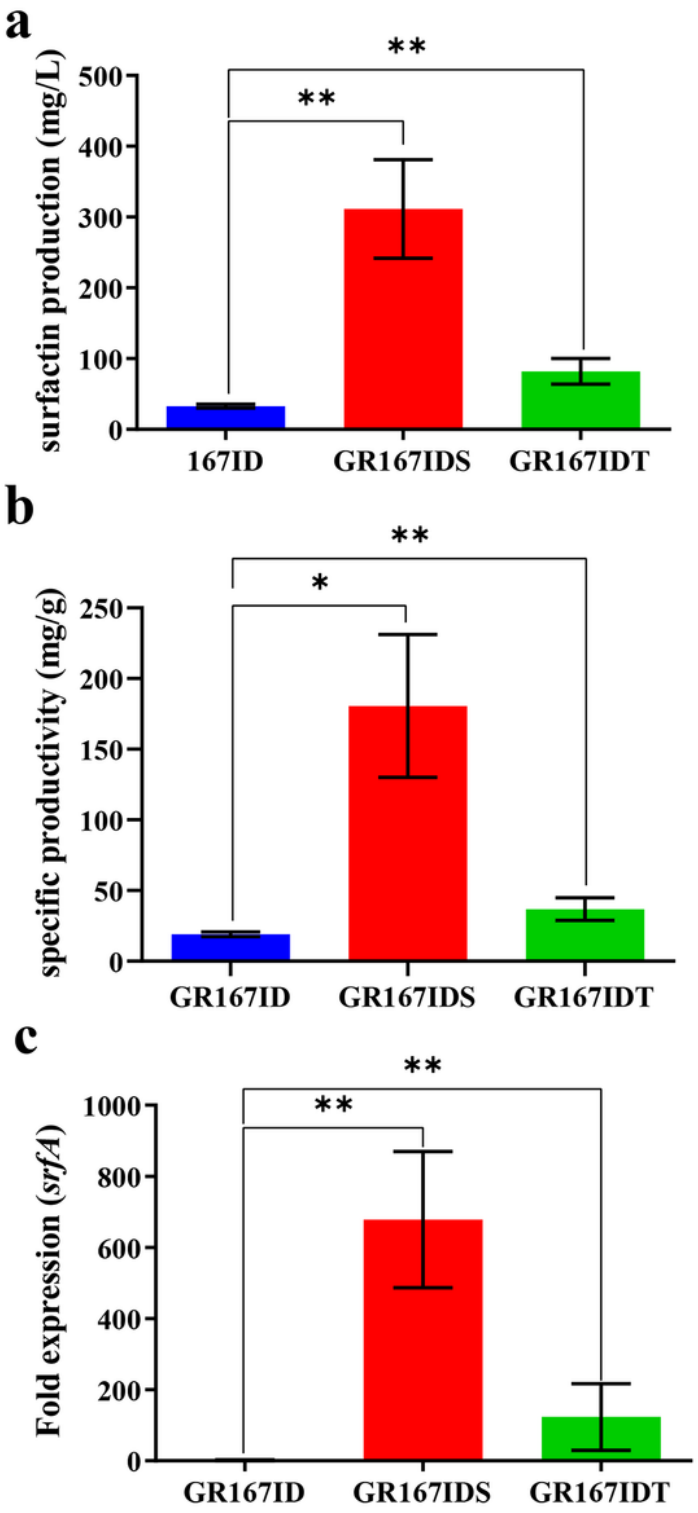

Figure 6

Surfactin production by GR167ID, GR167IDS and GR167IDT, and transcriptional levels of srfA operon in the strains. a Surfactin production; b specific productivity of surfactin (mg/g, the ratio of surfactin to CDW); c transcriptional levels of srfA operon quantified via qPCR (the transcriptional level of srfA operon in GR167ID was set as 1). Values denote mean ± SD of triplicates (*P < 0.05, **P < 0.01)

Supplementary Files

This is a list of supplementary files associated with this preprint. Click to download.

- supplementarymaterial.docx